

Theory of thin-skin eddy-current interaction with surface cracks

N. Harfield^{a)} and J. R. Bowler

Department of Physics, University of Surrey, Guildford, Surrey GU2 5XH, United Kingdom

(Received 27 May 1997; accepted for publication 14 July 1997)

Eddy-current non-destructive evaluation is commonly performed at relatively high frequencies at which the skin depths are significantly smaller than the dimensions of a typical crack. A thin-skin analysis of eddy currents is presented in which the electromagnetic fields on the crack faces are described in terms of a potential which obeys a two-dimensional Laplace equation. Solutions of this equation for defects in both magnetic and non-magnetic materials are determined by applying thin-skin boundary conditions at the crack perimeter. The impedance change of an eddy-current coil due to the defect is then calculated by numerical evaluation of one-dimensional integrals over the line of the crack mouth, the impedance integrals having been derived with the aid of a reciprocity relationship. Theoretical predictions are compared with experimental data for long, uniformly deep slots in aluminium and mild steel and good agreement between theory and experiment is obtained.

© 1997 American Institute of Physics. [S0021-8979(97)06920-X]

I. INTRODUCTION

In eddy-current non-destructive evaluation (NDE), the presence of a defect in a metal component is indicated by a change in the impedance of a probe. The change in probe impedance due to the interaction between eddy currents and the flaw can be predicted theoretically from the electromagnetic field. Here, the field at a crack due to a time-harmonic excitation by an induction coil is calculated in terms of a single scalar potential which obeys a two-dimensional Laplace equation in a domain corresponding to the crack surface. A solution is found by applying suitable boundary conditions and the coil impedance change due to the crack is calculated from the potential.

Although the surface potential used in the present formulation satisfies the Laplace equation at an arbitrary frequency, the boundary conditions used to determine the solution are restricted to the thin-skin regime. In this regime, the skin depth, δ , given by

$$\delta = \left(\frac{2}{\omega \mu_0 \mu_r \sigma} \right)^{1/2}, \quad (1)$$

is substantially smaller than the depth and length of the crack. It is estimated that reasonably accurate predictions can be made with the restricted boundary conditions provided the crack depth and length are greater than approximately three skin depths. Crack inspection that conforms to this condition is very common in practice because the probe sensitivity is likely to decrease as the frequency is lowered. A theoretical model valid in the thin-skin regime is therefore widely applicable both to the evaluation of crack signals in ferromagnetic steels and to high-frequency testing of non-magnetic materials.

The permeability of the material has a strong influence on the impedance change of the coil. This is clearly demonstrated in Figure 1, where predictions of coil impedance change as a function of frequency are shown for a coil centred over two identical long slots, one in a non-magnetic test

piece and the other in a test piece of relative permeability 100. These results indicate that the response from cracks in ferromagnetic materials differs in magnitude and frequency variation from that of cracks in non-ferromagnetic materials of similar conductivity.

Previously, a number of approaches have been taken in solving for the electromagnetic field at the crack in the thin-skin regime. These developments include the work of Auld *et al.*,¹ who considered cracks in aluminium alloys, and Lewis *et al.*² who were mainly concerned with flaws in ferromagnetic steels. A common feature of these studies is the use of the two-dimensional Laplace equation. Their distinctive theoretical aspects stem from the boundary conditions that are applied in obtaining the solution. The calculations for cracks in aluminium were performed using Auld's approximation,^{1,3} in which it is assumed that the external magnetic field tangential to the conductor surface is undisturbed by the crack. The approximation is reasonable provided that the ratio of the coil diameter to the crack depth is not too small, but this limitation leaves room for improvements in the predictions. In magnetic materials, the field in the vicinity of a crack is markedly different to that in aluminium since the magnetic field tangential to and at the surface of the conductor is perturbed significantly. The perturbed magnetic field at the crack mouth has been taken into account by Lewis *et al.*^{2,4} by deriving a boundary condition using a flux conservation argument applied to a region around the opening. The resulting theory is applicable to materials of arbitrary relative permeability.

In an earlier analysis of the field at cracks in magnetic materials by Collins *et al.*⁵ attention was focused on the line boundary between the conductor surface and the crack face. At this boundary, referred to as the fold line, the normal component of the current and the normal magnetic flux are deemed to be continuous. This implies that a complex potential representing the field in the surface plane and on the crack face is analytically continuous at the fold line. Consequently, the problem domain consists of a half plane representing half of the conductor surface adjoining one crack face unfolded into a common plane. A solution in this do-

^{a)}Electronic mail: n.harfield@surrey.ac.uk

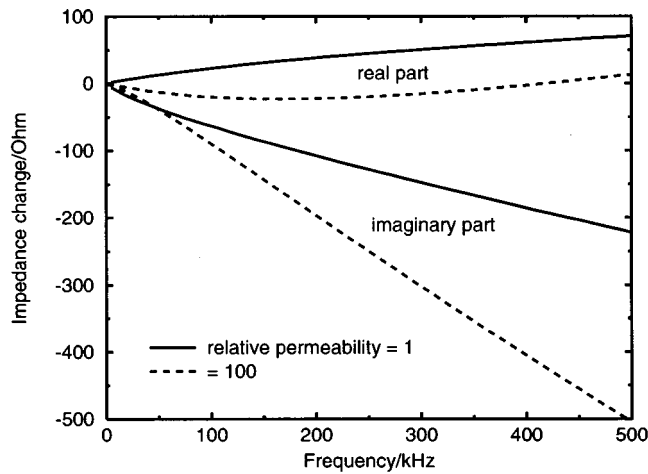


FIG. 1. Predicted impedance change for two identical long slots, one in a non-magnetic material and one in a material with $\mu_r = 100$. Apart from the value of μ_r , the parameters used in these predictions are given in the last column of Table I.

main corresponds to a surface potential that can be measured directly using contacting electrodes. The continuity condition is likely to be accurate for cracks of finite gape in materials of high permeability but the implication of later work is that the approach represents the high permeability limit of a more general theory.²

In the present study, the required boundary condition at the crack mouth is determined as a limiting case of an expression valid at arbitrary frequency and permeability. In order to improve on Auld's approximation, the perturbation of the surface magnetic field by the crack is taken into account. The resulting expressions are comparable with, but differ in detail from, those of Ref. 4.

In the thin-skin regime, calculations can be ordered in terms of the small parameter $1/ik$, where k is a complex wave number given by

$$k = \frac{1+i}{\delta}. \quad (2)$$

In particular, it is found that the coil impedance change, ΔZ , due to a flaw can be expressed as the following power series,

$$\Delta Z = Z^s \left[c_{-2} \left(\frac{1}{ik} \right)^{-2} + c_{-1} \left(\frac{1}{ik} \right)^{-1} + c_0 \left(\frac{1}{ik} \right)^0 + \dots \right], \quad (3)$$

where Z^s is a real normalising factor and the c_i are real coefficients. For cracks whose dimensions are an order of magnitude or more greater than δ , only the first two terms in Eq. (3) are required to represent ΔZ to a reasonable accuracy. The second and third terms of the above series are given by Kahn *et al.*⁶ for the two-dimensional thin-skin problem of eddy-current interaction with a long crack of uniform depth and negligible opening. The first term in the above series, a purely imaginary term, is missing from the Kahn expression for impedance because it represents the effect of crack opening which was not originally considered by Kahn *et al.*⁶ The imaginary term is associated with the electromagnetic energy stored in the crack volume. The second

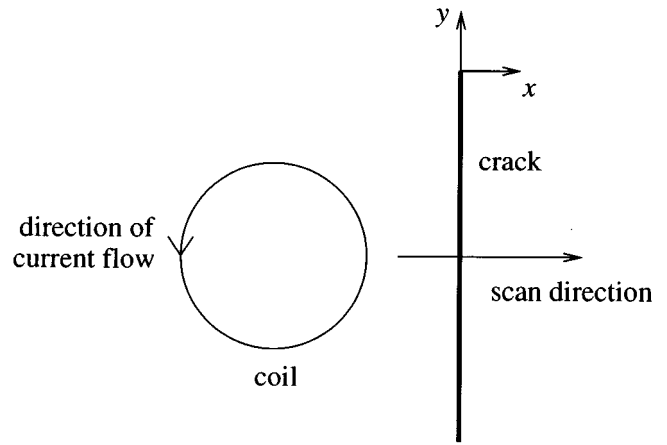


FIG. 2. Plan schematic view of an eddy-current inspection.

term is a surface effect and the third, purely resistive term, is due to the special behavior of the field at the crack mouth and edge. Auld refers to the edge and mouth impedance contributions as the Kahn terms. An improved analysis of these contributions has been given by Harfield and Bowler.⁷

In three-dimensional problems, it is not necessarily desirable to restrict the solution in such a way that the coefficients in the impedance expression are real. This is because a precise adherence to a strictly ordered expansion makes the analysis somewhat cumbersome. For example, in defining an unperturbed field, it is preferable to use the exact integral expressions available from the work of Dodd and Deeds,⁸ rather than a more awkward power series decomposition of the expressions.

In the present study of the three-dimensional thin-skin crack problem, the impedance contributions corresponding to the terms of Eq. (3) are derived for an arbitrary crack shape. Impedance predictions are then compared with experiments on long slots of uniform depth. For cracks whose depths are only a few times greater than δ , the third term in Eq. (3) is significant and, since it is related to the non-thin-skin behavior of the fields near the crack perimeter, it has a larger effect as the skin depth is increased. The term has previously been evaluated approximately by Auld⁹ by weighting two-dimensional solutions for a long crack in a uniform incident field^{6,7} with the locally varying component of the magnetic field directed tangential to the crack perimeter. We discuss this term and propose a new approximate expression which conforms with reciprocity principles. Note that even for defects of depth 3δ , however, the contribution to $|\Delta Z|$ from the third term in Eq. (3) is typically only about 5%.

II. SYMMETRY CONSIDERATIONS

Consider a coil whose axis is offset from the crack plane, $x=0$, as shown in Figure 2. For such cases, the solution can be found as the averaged sum of solutions for the odd and even configurations shown in Figure 3. In these configurations, an image coil mirrors the real coil in the crack plane. In the even configuration, Figure 3(a), the current flows in the same sense in each coil giving rise to an

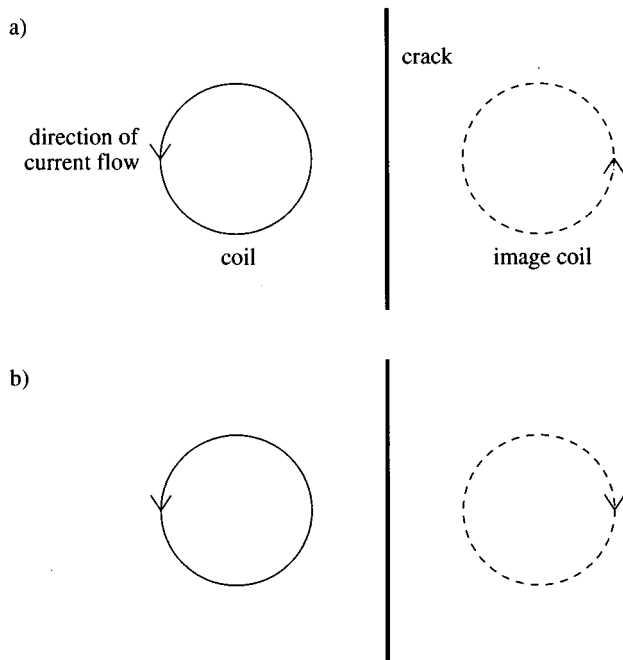


FIG. 3. The averaged sum of solutions for (a) odd and (b) even configurations gives the solution for a coil whose axis is offset from the plane of the crack.

electric field whose x component is even with respect to the x coordinate. In the odd configuration, the current in the image coil flows in the opposite sense to that in the real coil and the x component of the unperturbed electric field, the component normal to the crack plane, is odd in x .

An open narrow crack in a metal having a permeability greater than that of free space acts as barrier to the flow of current and a partial barrier to the magnetic flux. In the even system of Figure 3(a), the electromagnetic field can be viewed as interacting with the crack mainly through the electric field, since the component of the unperturbed magnetic field normal to the defect plane is zero. In the odd system of Figure 3(b), the converse is true; the electromagnetic field interaction can be viewed as magnetic since the component of the unperturbed electric field normal to the defect plane is zero.

For cracks in non-magnetic materials, and for cracks with a small opening in magnetic materials, the magnetic interaction is negligible. In these cases the problem can be solved purely in terms of the even configuration of Figure 3(a), which describes the flow of induced current around the defect. For a coil whose axis is centred over the defect, the problem can also be solved in terms of the even configuration since, by symmetry, the component of the magnetic field perpendicular to the defect plane is zero. If, however, there is a significant air gap between the faces of a crack in a magnetic material, and the coil axis is offset from the crack plane, then there may be a substantial magnetic interaction. This interaction is strengthened if the ratio of the material permeability to that of the defect is increased or if the size of the defect gape is increased, but, in most cases, its effect is still small when compared with the effect of the electric field

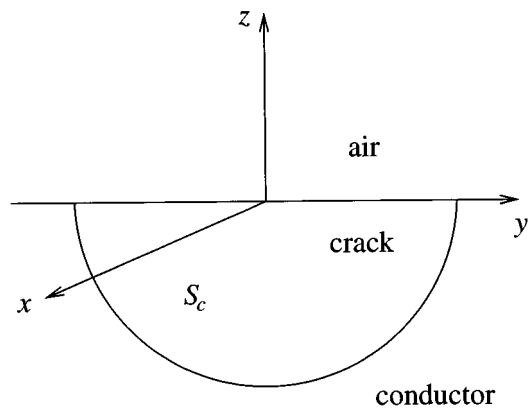


FIG. 4. A surface crack in a conducting half space.

perturbation. Since the magnetic field perturbation is significant only for coils offset from defects of substantial gape in highly permeable materials, we proceed to solve the problem in terms of the even configuration of Figure 3(a) alone, in which the electric interaction dominates.

III. SCALAR FORMULATION

A. Surface potential

Consider the planar crack in a conductor whose surface is in the plane $z=0$, Figure 4. It is assumed that the electromagnetic field varies as the real part of $\exp(-i\omega t)$, that the material properties are linear, that the displacement current is negligible and that the conductor is sufficiently thick to behave as a half space. For the purpose of calculating the fields it is also assumed that the crack is ideal in that it has a negligible opening but forms a perfect barrier to the flow of current. The calculation of the impedance change due to the defect presented in Section IV does, however, allow for the possibility of finite gape.

The field calculation proceeds by decomposing the electric and magnetic fields in the conductor, $z < 0$, into transverse electric (TE) and transverse magnetic (TM) components:¹⁰

$$\mathbf{E}(\mathbf{r}) = i\omega\mu_0\mu_r[\nabla \times \hat{x}\psi'(\mathbf{r}) - \nabla \times \nabla \times \hat{x}\psi''(\mathbf{r})], \quad z < 0, \quad (4)$$

$$\mathbf{H}(\mathbf{r}) = \nabla \times \nabla \times \hat{x}\psi'(\mathbf{r}) - k^2\nabla \times \hat{x}\psi''(\mathbf{r}), \quad z < 0, \quad (5)$$

where the preferred direction, \hat{x} , is normal to the crack plane, ψ' is the TE potential, ψ'' is the TM potential and $k^2 = i\omega\mu_r\mu_0\sigma$. By substituting Eqs. (4) and (5) into the electromagnetic field equations, it can be shown that the TE and TM potentials satisfy¹⁰

$$(\nabla^2 + k^2)\nabla_x^2\psi'(\mathbf{r}) = 0, \quad (6)$$

$$(\nabla^2 + k^2)\nabla_x^2\psi''(\mathbf{r}) = 0, \quad (7)$$

where $\nabla_x = \nabla - \hat{x}\partial/\partial x$ is the transverse gradient with respect to the x direction. Although the potentials are not coupled through their governing equations, they are related through the interface conditions at the surface of the conductor. This interdependence is expressed in terms of 2×2 matrices of

reflection coefficients and transmission coefficients, given in the Appendix, which account for the fact that a TM field incident on the interface reflects and transmits both TE and TM modes, the same being true of an incident TE mode.

In a half-space problem formulated using Hertz potentials, it is usual to choose the preferred direction as the normal to the interface. By following this standard formulation the coupling between potentials through the interface conditions is avoided. Although the present choice of preferred direction leads to coupled interface conditions, the chosen modes are decoupled at the crack surface. In fact, the TE mode does not interact directly with an ideal crack at all. Instead, it is perturbed indirectly via its link with the TM mode at the surface of the conductor. Because direct TE interaction with the crack is absent, the TE potential and its gradients are continuous at the crack plane. In contrast, the TM potential is subject to a direct crack-field interaction and therefore has a discontinuity at the crack.

In order to examine the discontinuity of the TM Hertz potential, the properties of the electromagnetic field at the crack are reviewed.¹¹ Firstly, it is noted that the tangential magnetic field is continuous at an ideal crack, a condition that can be written as

$$\mathbf{H}_t(\mathbf{r}_+) - \mathbf{H}_t(\mathbf{r}_-) = 0, \quad (8)$$

where the \pm subscripts refer to limiting values of the coordinate as the crack plane is approached from one side or the other and the subscript t denotes components tangential to the crack. In the absence of direct TE interaction, the magnetic field continuity condition applies to the TM contribution alone and implies that

$$\psi''(\mathbf{r}_+) - \psi''(\mathbf{r}_-) = 0. \quad (9)$$

Thus the TM potential itself is continuous at the crack surface S_c .

The tangential electric field has a discontinuity at the crack which can be expressed as the gradient of a scalar function,¹¹ a relationship that is written

$$\mathbf{E}_t(\mathbf{r}_+) - \mathbf{E}_t(\mathbf{r}_-) = -\frac{1}{\sigma} \nabla_t p(\mathbf{r}), \quad \mathbf{r} \in S_c, \quad (10)$$

where $p(\mathbf{r})$ is the equivalent source density of the crack represented by a layer of electric current dipoles orientated normal to the crack surface S_c . Since the jump in the electric field is solely due to the TM mode, it can be seen from the form of the TM contribution in Eq. (4) that

$$\left. \frac{\partial \psi''}{\partial x} \right|_{\mathbf{r}_+} - \left. \frac{\partial \psi''}{\partial x} \right|_{\mathbf{r}_-} = \frac{1}{k^2} p(\mathbf{r}), \quad \mathbf{r} \in S_c. \quad (11)$$

Hence the TM potential has a discontinuity in its normal gradient at the crack surface S_c .

Assuming that the crack is impenetrable to eddy currents, then the normal component of current at the crack surface is zero. For a crack in the yz plane, this leads to the condition

$$\mathbf{E}(\mathbf{r}) \cdot \hat{x} = 0, \quad \mathbf{r} \in S_c. \quad (12)$$

Applying Eq. (12) to Eq. (4) shows that

$$\nabla_x^2 \psi''(\mathbf{r}) = 0, \quad \mathbf{r} \in S_c, \quad (13)$$

where ∇_x^2 is the Laplacian operator transverse to x . Note that Eq. (13) shows that $\psi''(\mathbf{r})$ satisfies the surface Laplace equation regardless of the frequency.

Having established the general behavior of the potentials at the crack surface, an integral equation will be given which determines $\psi''(\mathbf{r})$ at an arbitrary frequency. Although it is possible to use this equation as the basis for computing numerical solutions, it will be used here for the more limited purpose of defining a crack mouth boundary condition in order that the Laplace equation, Eq. (13), can be solved. For notational convenience write

$$\psi = -k^2 \psi''. \quad (14)$$

Then, in the presence of an ideal crack, ψ satisfies

$$\psi(\mathbf{r}) = \psi^{(i)}(\mathbf{r}) + \int_{S_c} G(\mathbf{r}, \mathbf{r}') p(\mathbf{r}') dS', \quad \mathbf{r} \in S_c, \quad (15)$$

where the superscript (i) denotes the incident, or unperturbed, field. The Green's function for the TM potential in a half-space conductor, derived in the Appendix as $G_{22}(\mathbf{r}, \mathbf{r}')$, is given by

$$G(\mathbf{r}, \mathbf{r}') = \frac{e^{ik|\mathbf{r}-\mathbf{r}'|}}{4\pi|\mathbf{r}-\mathbf{r}'|} + \frac{e^{ik|\mathbf{r}-\mathbf{r}''|}}{4\pi|\mathbf{r}-\mathbf{r}''|} + \frac{1}{k^2} \frac{\partial^2}{\partial y^2} \times U(x-x', y-y', z+z'), \quad (16)$$

where $\mathbf{r}'' = \mathbf{r}' - 2\hat{z}z'$ is the image point and

$$U(x, y, z) = \frac{\mu_r k^4}{(2\pi)^2} \int_{-\infty}^{\infty} \int_{-\infty}^{\infty} \frac{1}{u^2 - k^2} \left(\frac{1}{\kappa} - \frac{\mu_r}{\gamma} \right) \times \frac{1}{[(\mu_r^2 - 1)\kappa^2 + k^2]} e^{-\gamma z + iux + ivy} dudv, \quad (17)$$

where $\gamma = (u^2 + v^2 - k^2)^{1/2}$ and $\kappa = (u^2 + v^2)^{1/2}$.

Equation (15) could presumably be derived with the aid of Green's second theorem applied to a surface surrounding the crack. However, there are major complications involved in such a derivation because the crack intersects the surface of the conductor where the scalar fields are coupled. Instead of attempting a first principles derivation, our justification for using Eq. (15) relies on an equivalence between the present scalar representation of the field and a vector potential formulation given previously.¹² The connection is made by noting that the x component of the current density due to the perturbed field at a crack face is equal and opposite to the unperturbed current density. Writing this as

$$\nabla_x^2 \psi^{(s)}(\mathbf{r}) = J_x^{(i)}(\mathbf{r}), \quad \mathbf{r} \in S_c, \quad (18)$$

where the superscript (s) denotes the perturbed field, and, noting the correspondence with Eq. (17) of Ref. 12, allows an identification of an integral expression for $\psi^{(s)}(\mathbf{r})$ from which Eq. (15) follows.

B. Boundary conditions

While ψ satisfies the surface Laplace equation given in Eq. (13) at arbitrary frequency, the boundary conditions at the crack edge and mouth given in this section are valid only in the thin-skin limit. In the thin-skin regime, the component of the magnetic flux density normal to the crack edge is zero.⁴ From this we deduce that

$$\mathbf{H}_{\text{TM}}(\mathbf{r}_e) \cdot \hat{n} = 0, \quad (19)$$

where \mathbf{r}_e denotes the coordinate of a point at the crack edge and \hat{n} is a unit vector pointing outward from the crack edge and lying in the crack plane. Noting that

$$\mathbf{H}_{\text{TM}}(\mathbf{r}) = \nabla \times \hat{x} \psi, \quad (20)$$

and applying Eq. (19) to Eq. (20) shows that on the crack edge

$$\psi(\mathbf{r}_e) = 0, \quad (21)$$

where an arbitrary integration constant has been set to zero.

At the crack mouth, a boundary condition is applied which is derived from the magnetic field transverse to the surface of the conductor. In general the y component of this field can be expressed as

$$H_{y\text{TM}}(\mathbf{r}_m) = H_{y\text{TM}}^{(i)}(\mathbf{r}_m) + H_{y\text{TM}}^{(s)}(\mathbf{r}_m), \quad (22)$$

where \mathbf{r}_m denotes the coordinate of a point at the crack mouth. In dealing with cracks in non-magnetic materials, Auld^{1,9} neglects the term $H_{y\text{TM}}^{(s)}(\mathbf{r}_m)$ which implies that the perturbation of the y component of the magnetic field due to the crack is negligible at the crack mouth. By retaining the effect of the scattered magnetic field in the boundary condition, it is found that an additional impedance contribution arises which is in fact of higher order than that of the Kahn terms. In the case of magnetic materials, the effect of the scattered magnetic field on the mouth boundary condition is somewhat larger than for non-magnetic material and therefore cannot be ignored.

In the thin-skin regime the kernel of Eq. (15) is highly localised such that in the limit its effect can be represented by a delta function.¹² The localization of the kernel has been used to show that

$$p(\mathbf{r}) \approx -2ik\psi(\mathbf{r}), \quad (23)$$

in the thin-skin limit.¹² Although the functional form of $p(\mathbf{r})$ and $\psi(\mathbf{r})$ are different at the mouth of the crack, Eq. (23) approximates the magnitude of the dipole density in that region.

Differentiating Eq. (15) with respect to z , using Eq. (23) and restricting \mathbf{r} to \mathbf{r}_m gives

$$\left. \frac{\partial \psi(\mathbf{r})}{\partial z} \right|_{\mathbf{r}=\mathbf{r}_m} = \left. \frac{\partial \psi^{(i)}(\mathbf{r})}{\partial z} \right|_{\mathbf{r}=\mathbf{r}_m} + \frac{2}{ik} \int_{-c/2}^{c/2} \frac{\partial^2}{\partial y'^2} \times U(0, y-y', 0) \psi(0, y', 0) dy', \quad (24)$$

where c is the crack length. The integration with respect to z' has been carried out by assuming that $\psi(0, y', z')$ varies slowly with z' and is therefore roughly constant over the effective range of the kernel in the z direction. Equation (24) is the thin-skin equivalent of Eq. (22).

To summarize, the TM potential at the crack surface has been shown to satisfy a two-dimensional Laplace equation, Eq. (13), regardless of the frequency or skin depth. This equation will be solved by applying boundary conditions at the crack edge and mouth, Eqs. (21) and (24), respectively, which are valid for small skin depths.

C. Magnetic field

In order to evaluate the impedance due to an open crack, the total magnetic field at the crack mouth in the plane of the surface of the conductor is required. The field in this region is approximated by the magnetic field at the line of the crack mouth for a closed crack. The magnetic field can be written as a sum of the field incident from the coil and an integral form of that scattered by the defect:

$$H_y(\mathbf{r}) = H_y^{(i)}(\mathbf{r}) + \int_{S_c} g(\mathbf{r}, \mathbf{r}') p(\mathbf{r}') dS', \quad \mathbf{r} \in S_c, \quad (25)$$

where p is an equivalent current dipole density at the crack. This relationship is found from the corresponding integral equation for the electric field.¹¹ The half-space Green' function is given by

$$g(\mathbf{r}, \mathbf{r}') = \frac{\partial}{\partial z} \left[\frac{e^{ik|\mathbf{r}-\mathbf{r}'|}}{4\pi|\mathbf{r}-\mathbf{r}'|} + \frac{e^{ik|\mathbf{r}-\mathbf{r}''|}}{4\pi|\mathbf{r}-\mathbf{r}''|} - \frac{1}{k^2} \frac{\partial^2}{\partial y'^2} \times V(x-x', y-y', z+z') \right], \quad (26)$$

where $\mathbf{r}'' = \mathbf{r}' - 2\hat{z}z'$ is the image point and

$$V(x, y, z) = \frac{1}{k^2} \nabla_x^2 U(x, y, z) = \frac{\mu_r k^2}{(2\pi)^2} \int_{-\infty}^{\infty} \int_{-\infty}^{\infty} \left(\frac{1}{\kappa} - \frac{\mu_r}{\gamma} \right) \times \frac{1}{[(\mu_r^2 - 1)\kappa^2 + k^2]} e^{-\gamma z + iux + ivy} dudv. \quad (27)$$

Using the thin-skin relation between p and ψ given in Eq. (23) it is found from Eq. (25) that

$$H_y(\mathbf{r}_m) = H_y^{(i)}(\mathbf{r}_m) - \frac{2}{ik} \int_{-c/2}^{c/2} \frac{\partial^2}{\partial y'^2} \times V(0, y-y', 0) \psi(0, y', 0) dy', \quad (28)$$

where \mathbf{r}_m denotes the coordinate of a point at the crack mouth and c is the crack length. Again, the integration with respect to z' has been carried out by assuming that $\psi''(0, y', z')$ varies slowly with z' and is therefore roughly constant over the effective range of the kernel in the z direction.

D. Fourier representation

The kernel U in the integral of Eq. (24) can be represented in terms of its Fourier transform in y :

$$\tilde{U}(x, v, z) = \int_{-\infty}^{\infty} U(x, y, z) e^{-ivy} dy. \quad (29)$$

From Eq. (17) we then have, putting $\tilde{U}(v) = \tilde{U}(0, v, 0)$,

$$\begin{aligned} \tilde{U}(v) &= \frac{\mu_r k^4}{2\pi} \int_{-\infty}^{\infty} \frac{1}{u^2 - k^2} \left(\frac{1}{\kappa} - \frac{\mu_r}{\gamma} \right) \\ &\quad \times \frac{1}{[(\mu_r^2 - 1)\kappa^2 + k^2]} du. \end{aligned} \quad (30)$$

The integral of Eq. (30) can be evaluated by splitting the integrand using partial fractions and then using the standard form

$$\begin{aligned} F(\alpha, \beta) &= \int_{-\infty}^{\infty} \frac{du}{(u^2 - \alpha^2)\sqrt{u^2 + (\beta^2 - \alpha^2)}} \\ &= \frac{1}{\alpha\beta} \ln \left(\frac{\alpha - \beta}{\alpha + \beta} \right). \end{aligned} \quad (31)$$

The resulting expression for $\tilde{U}(v)$ is

$$\begin{aligned} \tilde{U}(v) &= \frac{\mu_r}{2\pi[(\mu_r^2 - 1)w^2 + \mu_r^2]} \left\{ \frac{\mu_r}{w} \ln \left(\frac{1+w}{1-w} \right) \right. \\ &\quad - \frac{1}{\sqrt{1+w^2}} \ln \left(\frac{1+\sqrt{1+w^2}}{1-\sqrt{1+w^2}} \right) \\ &\quad + \frac{\mu_r^2 - 1}{\sqrt{(\mu_r^2 - 1)w^2 + 1}} \left[\ln \left(\frac{\sqrt{(\mu_r^2 - 1)w^2 + 1} + \mu_r}{\sqrt{(\mu_r^2 - 1)w^2 + 1} - \mu_r} \right) \right. \\ &\quad \left. \left. - \ln \left(\frac{\sqrt{(\mu_r^2 - 1)w^2 + 1} + 1}{\sqrt{(\mu_r^2 - 1)w^2 + 1} - 1} \right) \right] \right\}, \end{aligned} \quad (32)$$

where $w = v/k$. Equation (32) is valid for all μ_r . For highly permeable materials, the last two terms in Eq. (32) dominate and $\tilde{U}(v)$ may be approximated by¹³

$$\tilde{U}(v)_{\mu_r \gg 1} \approx -\frac{\mu_r}{2\pi\sqrt{\zeta^2 + 1}} \ln \left(\frac{1 + \sqrt{\zeta^2 + 1}}{1 - \sqrt{\zeta^2 + 1}} \right), \quad (33)$$

where $\zeta = \mu_r v/k$. For non-permeable materials, the last two terms in Eq. (32) vanish and

$$\begin{aligned} \tilde{U}(v)_{\mu_r = 1} &= \frac{1}{2\pi} \left[\frac{1}{w} \ln \left(\frac{1+w}{1-w} \right) \right. \\ &\quad \left. - \frac{1}{\sqrt{1+w^2}} \ln \left(\frac{1+\sqrt{1+w^2}}{1-\sqrt{1+w^2}} \right) \right]. \end{aligned} \quad (34)$$

This term, used in Eq. (24), provides a correction to Auld's theory in which the scattered tangential magnetic field at the conductor surface is assumed to be zero.^{1,3,9}

In a similar manner, the kernel V in the integral of Eq. (28) can be represented algebraically in terms of its Fourier transform in y :

$$\tilde{V}(x, v, z) = \int_{-\infty}^{\infty} V(x, y, z) e^{-ivy} dy. \quad (35)$$

From Eq. (27) we have, putting $\tilde{V}(v) = \tilde{V}(0, v, 0)$,

$$\tilde{V}(v) = \frac{\mu_r k^2}{2\pi} \int_{-\infty}^{\infty} \left(\frac{1}{\kappa} - \frac{\mu_r}{\gamma} \right) \frac{1}{[(\mu_r^2 - 1)\kappa^2 + k^2]} du, \quad (36)$$

which can be integrated to give

$$\begin{aligned} \tilde{V}(v) &= -\frac{\mu_r}{2\pi} \left[\ln \left(\frac{\sqrt{(\mu_r^2 - 1)w^2 + 1} + \mu_r}{\sqrt{(\mu_r^2 - 1)w^2 + 1} - \mu_r} \right) \right. \\ &\quad \left. - \frac{1}{\sqrt{(\mu_r^2 - 1)w^2 + 1}} \ln \left(\frac{\sqrt{(\mu_r^2 - 1)w^2 + 1} + 1}{\sqrt{(\mu_r^2 - 1)w^2 + 1} - 1} \right) \right]. \end{aligned} \quad (37)$$

Equation (37) is valid for all μ_r . For highly permeable materials, Eq. (37) can be approximated by

$$\tilde{V}(v)_{\mu_r \gg 1} \approx \frac{\mu_r}{2\pi\sqrt{\zeta^2 + 1}} \ln \left(\frac{1 + \sqrt{\zeta^2 + 1}}{1 - \sqrt{\zeta^2 + 1}} \right). \quad (38)$$

Note that this term is equal and opposite to the high permeability form of $\tilde{U}(v)$ given in Eq. (33). For $\mu_r = 1$, the integral of Eq. (36) can be evaluated using the standard form

$$\int \frac{du}{\sqrt{u^2 + \alpha^2}} = \ln(u + \sqrt{u^2 + \alpha^2}), \quad (39)$$

giving,

$$\tilde{V}(v)_{\mu_r = 1} = -\frac{1}{\pi} \ln \left(\frac{w}{\sqrt{w^2 - 1}} \right). \quad (40)$$

Equations (37)–(40) are used in Eq. (28) to evaluate the surface magnetic field as required for the calculation of probe impedance.

IV. PROBE IMPEDANCE

Define the impedance change in a coil due to a defect as

$$\Delta Z = Z - Z_0, \quad (41)$$

where Z is the impedance of the coil in the presence of the flawed conductor and Z_0 is the coil impedance in the presence of a similar but unflawed conductor. The impedance change can be written as the following integral over the coil region:

$$\Delta Z = - \int_{\Omega} [\mathbf{E} - \mathbf{E}^{(i)}] \cdot \mathbf{J} dV \quad (42)$$

for unit coil current. Equation (42) is transformed to a surface integral by noting that

$$(\nabla \times \nabla \times - k^2) \mathbf{E} = i\omega\mu\mathbf{J}, \quad (43)$$

$$(\nabla \times \nabla \times - k^2) \mathbf{E}^{(i)} = i\omega\mu\mathbf{J}, \quad (44)$$

and putting $\mathbf{a} = \mathbf{E}^{(i)}$ and $\mathbf{b} = \mathbf{E}/i\omega\mu$ in the identity

$$\begin{aligned} &\int [\mathbf{b} \cdot \nabla \times \nabla \times \mathbf{a} - \mathbf{a} \cdot \nabla \times \nabla \times \mathbf{b}] dV \\ &= \int [\mathbf{a} \times (\nabla \times \mathbf{b}) - \mathbf{b} \times (\nabla \times \mathbf{a})] \cdot d\mathbf{S}. \end{aligned} \quad (45)$$

This gives

$$\Delta Z = - \int_S [\mathbf{E}^{(i)} \times \mathbf{H} - \mathbf{E} \times \mathbf{H}^{(i)}] \cdot \hat{n} dS, \quad (46)$$

where \hat{n} is an outward pointing unit vector normal to the surface S which encloses the coil. In order to calculate ΔZ , Eq. (46) is transformed so that the impedance is expressed in terms of quantities which are either known or are easily derived from the surface potential. This is accomplished by eliminating the perturbed and unperturbed electric fields as follows. Choose the surface S so that it coincides with the conductor surface and then split the integral of Eq. (46) into two parts, an integral over the crack mouth, S_m , and an integral over the unflawed conductor surface, $S - S_m$:

$$\begin{aligned} \Delta Z = & \int_{S_m} [\mathbf{E}^{(i)} \times \mathbf{H} - \mathbf{E} \times \mathbf{H}^{(i)}] \cdot \hat{z} dS \\ & + \int_{S - S_m} [\mathbf{E}^{(i)} \times \mathbf{H} - \mathbf{E} \times \mathbf{H}^{(i)}] \cdot \hat{z} dS. \end{aligned} \quad (47)$$

The first term in Eq. (47), written as

$$Z_S = \int_{S_m} [\mathbf{E}^{(i)} \times \mathbf{H}] \cdot \hat{z} dS, \quad (48)$$

is evaluated first, followed by a strictly thin-skin evaluation of the second term in Eq. (47), denoted

$$Z_F = - \int_{S_m} [\mathbf{E} \times \mathbf{H}^{(i)}] \cdot \hat{z} dS. \quad (49)$$

Finally, the integral over $S - S_m$ is evaluated approximately along with terms of the same order in the integral of $\mathbf{E} \times \mathbf{H}^{(i)}$ over S_m . The aim is to find the total impedance change due to cracks with finite opening by using field solutions that have been found for cracks of zero opening. Inevitably this involves further approximations, particularly in dealing with the smaller terms, but the results show that good predictions are possible even in the absence of a rigorous solution to the open crack problem.

A. Evaluation of Z_S

In the thin-skin regime, a relationship between the transverse field components at the conductor surface can be derived from Maxwell's equations by assuming that the field varies much more rapidly in the direction normal to the boundary than in the direction tangential to the boundary. This relationship, known as the surface impedance boundary condition, is expressed in terms of the unperturbed field as

$$\hat{z} \times \mathbf{E}_t^{(i)} = \frac{ik}{\sigma} \mathbf{H}_t^{(i)}, \quad (50)$$

where the subscript t refers to transverse field components. Using the fact that

$$H_x(0, y, 0) = 0, \quad (51)$$

as required by the symmetry argument of Section II, and applying Eq. (50) to Eq. (48) gives

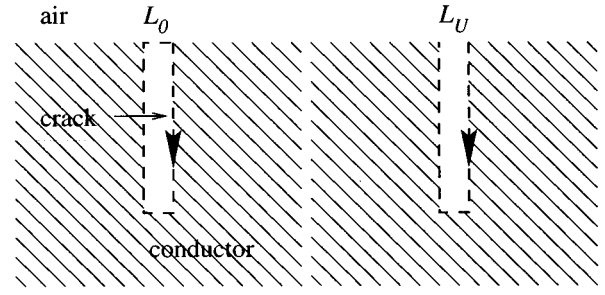


FIG. 5. Paths L_0 and L_U .

$$Z_S = \frac{ika}{\sigma} \int_{-c/2}^{c/2} H_y^{(i)}(0, y, 0) H_y(0, y, 0) dy, \quad (52)$$

where a is the crack gape. Integration with respect to x has been carried out by assuming that the magnetic field approximates a linear function over the width of the crack opening.

Physically, Z_S describes the impedance change resulting from removal of part of the surface of the unflawed conductor on introducing the flaw. It can be calculated from a one-dimensional integral along the line of the crack mouth, as given in Eq. (52). The incident magnetic field required in Eq. (52) can be evaluated, for a coil with axis perpendicular to the conductor surface, using closed-form expressions⁸ and the y component of the total magnetic field can be calculated using Eq. (28). From Eq. (52) it is evident that Z_S contributes to ΔZ at the order of the second term in Eq. (3) and that the contribution vanishes as the gape tends to zero.

B. Evaluation of Z_F

We will evaluate the integral of Eq. (49) using the surface impedance boundary condition. This leads to contributions to ΔZ of the order of the first two terms in Eq. (3). The resulting expression, combined with Z_S , accurately expresses ΔZ at the order of the first two terms in Eq. (3).

The expression for Z_F given in Eq. (49) can be written in terms of field components which are either known or can be calculated by means of the following manipulation. Write

$$Z_F = - \int_{S_m} [\mathbf{H}^{(i)} \times \hat{z}] \cdot \mathbf{E} dS. \quad (53)$$

Again assuming that $H_x^{(i)}$ and $H_y^{(i)}$ are linear across the crack and making use of Eq. (51) allows Eq. (53) to be written

$$Z_F = - \int_{-c/2}^{c/2} H_y^{(i)}(0, y, 0) \left[\int_{-a/2}^{a/2} \mathbf{E}(x, y, 0) \cdot d\mathbf{x} \right] dy. \quad (54)$$

Now E_x is, by the definition of Eq. (4), expressed in terms of the TM potential alone. This means that

$$\mathbf{E} \cdot d\mathbf{x} = \mathbf{E}_{TM} \cdot d\mathbf{x} \quad (55)$$

and

$$Z_F = - \int_{-c/2}^{c/2} H_y^{(i)}(0, y, 0) \left[\int_{-a/2}^{a/2} \mathbf{E}_{TM}(x, y, 0) \cdot d\mathbf{x} \right] dy. \quad (56)$$

The line integral in square brackets will now be written as the difference between an integral which completely en-

closes the flaw, following path L_0 , and one which excludes the mouth region, following path L_U . Using the paths shown in Figure 5, write

$$\int_{-a/2}^{a/2} \mathbf{E}_{\text{TM}} \cdot d\mathbf{x} = \oint_{L_0} \mathbf{E}_{\text{TM}} \cdot d\mathbf{l} - \int_{L_U} \mathbf{E}_{\text{TM}} \cdot d\mathbf{l}. \quad (57)$$

Applying Stokes's theorem to the integral over L_0 and the surface impedance boundary condition to the integral over L_U gives

$$\begin{aligned} \int_{-a/2}^{a/2} \mathbf{E}_{\text{TM}} \cdot d\mathbf{x} &= i\omega\mu_0\mu_c \int_{z_e}^0 \int_{-a/2}^{a/2} H_{y\text{TM}}(x,y,z) dx dz \\ &+ \frac{2ik}{\sigma} \int_{z_e}^0 H_{y\text{TM}}(0,y,z) dz \\ &+ \frac{ik}{\sigma} \int_{-a/2}^{a/2} H_{r\text{TM}}(x,y,z_e) dx, \end{aligned} \quad (58)$$

where μ_c is the relative permeability of the material within the defect and $H_{r\text{TM}}$ denotes the component of \mathbf{H}_{TM} tangential to the edge. Assuming that these field components are uniform across the flaw, integration with respect to x gives

$$\begin{aligned} \int_{-a/2}^{a/2} \mathbf{E}_{\text{TM}} \cdot d\mathbf{x} &= \frac{1}{\sigma} \left(k^2 a \frac{\mu_c}{\mu_r} + 2ik \right) \int_{z_e}^0 H_{y\text{TM}}(0,y,z) dz \\ &+ \frac{ika}{\sigma} H_{r\text{TM}}(0,y,z_e). \end{aligned} \quad (59)$$

Writing $H_{y\text{TM}} = \partial\psi/\partial z$ and integrating with respect to z gives

$$\int_{z_e}^0 H_{y\text{TM}}(0,y,z) dz = \psi(0,y,0). \quad (60)$$

Expression (56) can finally be written in terms of the following one-dimensional integrals:

$$\begin{aligned} Z_F &= -\frac{1}{\sigma} \left(k^2 a \frac{\mu_c}{\mu_r} + 2ik \right) \int_{-c/2}^{c/2} H_y^{(i)}(0,y,0) \psi(0,y,0) dy \\ &- \frac{ika}{\sigma} \int_{-c/2}^{c/2} H_y^{(i)}(0,y,0) H_{r\text{TM}}(0,y,z_e) dy. \end{aligned} \quad (61)$$

As for Z_S , the incident field from the coil in the integrand of Eq. (61) can be calculated, for a coil with axis perpendicular to the conductor surface, using closed-form expressions.⁸ The potential ψ is obtained by solving the Laplace problem described in Section III and $H_{r\text{TM}}(0,y,z_e)$ can be found from the potential. The first term in Eq. (61) clearly contributes to ΔZ at the order of both the first and second terms in Eq. (3). The part which depends on k^2 is a volume-dependent contribution which vanishes as the crack gape tends to zero. The part which depends on k is related to current flow over the faces of the defect—the factor of 2 reflects the presence of the two crack faces. The second term in Eq. (61) contributes to ΔZ at the order of the second term in Eq. (3). It is related to the current flowing over the base of the defect and vanishes as the defect gape tends to zero.

C. Evaluation of Z_K

For defects whose dimensions are only a few times greater than δ , the third term in Eq. (3) is significant. Here, we propose an approximate form for this term which we denote Z_K after Kahn *et al.*,⁶ who first evaluated this term in the context of a long crack in a uniform field. The development is not strictly rigorous since the resulting expressions involve field values which are determined using thin-skin assumptions, such as the relationship between p and ψ of Eq. (23).

Kahn-level contributions arise from the integral of $\mathbf{E} \times \mathbf{H}^{(i)}$ over S_m and the integral over $S - S_m$ in Eq. (47). Consider firstly the contribution from the integral over $S - S_m$. This integral gives rise to two equal terms, one from the surface on each side of the crack. If the surface impedance boundary condition is used for \mathbf{E} as well as $\mathbf{E}^{(i)}$, the integral over $S - S_m$ vanishes but the boundary condition is not in fact valid in the region within a few skin depths of the crack opening. An improved approximation is obtained by adapting a local solution for the corner region of the two-dimensional long crack problem.⁷ From this problem it is evident that the x component of the electric field can be written as

$$E_x = \frac{ikH_y}{\sigma} \left[1 - k \int_{x-a/2}^{\infty} H_0^{(1)}(ku) du \right] \quad x \geq a/2, \quad (62)$$

which vanishes for $x = a/2$, as indeed it should.

Substituting Eqs. (50) and (62) into the second term in Eq. (47), using Eq. (51) and integrating with respect to x gives the following contribution to ΔZ :

$$-\frac{4}{\pi\sigma} \int_{-c/2}^{c/2} H_y^{(i)}(0,y,0) H_y(0,y,0) dy. \quad (63)$$

This Kahn term contributes at the third level in Eq. (3) and represents the effect of a highly localised corner field at the surface of the conductor close to the crack mouth. An equivalent term arises from the integration over the crack faces, along with a contribution due to local field variation at the crack edge.

Kahn-level contributions from the integral of $\mathbf{E} \times \mathbf{H}^{(i)}$ over S_m will now be determined. The development proceeds as for Z_F up to Eq. (57). For the integration over L_U , the surface impedance boundary condition is now modified to account for third order effects. The relationship is supplemented by terms representing the corner field, as in Eq. (62), and the edge field, as in Eq. (8) of Ref. 7. Hence for the local electric field near the crack mouth,

$$E_{z\text{TM}} = \frac{ikH_y}{\sigma} \left[1 - k \int_{-z}^{-\infty} H_0^{(1)}(ku) du \right], \quad (64)$$

and, approaching the edge of the crack,⁷

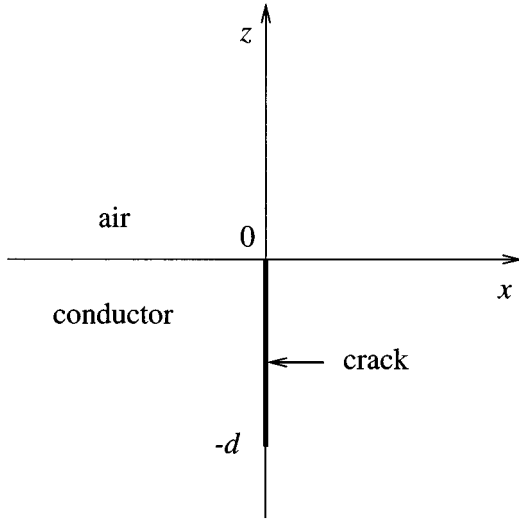


FIG. 6. A conducting half space containing a long, surface-breaking crack.

$$E_{z\text{TM}} = \frac{ikH_{r\text{TM}}}{\sigma} \left[1 - \operatorname{erfc}(-i\sqrt{ik(z \cos\theta + d)}) + \frac{i}{\sqrt{\pi}} \frac{e^{ik(z \cos\theta - z_e)}}{\sqrt{ik(z \cos\theta - z_e)}} \right], \quad (65)$$

where z_e is the coordinate of the crack edge and θ is the angle between the inwardly directed normal to the crack edge and \hat{z} . The first terms in Eqs. (64) and (65) represent the unmodified surface impedance boundary condition and give rise to the terms of order k in Z_F . The remaining terms represent the non-Laplacian, locally varying field. Integrating over L_U now gives rise to the following terms in addition to those of Eq. (58):

$$\frac{4}{\sigma\pi} H_{y\text{TM}}(0, y, 0) - \frac{1}{\sigma \cos\theta} H_{r\text{TM}}(0, y, z_e). \quad (66)$$

Combining the impedance contribution from these terms with that of Eq. (63) gives Z_K :

$$Z_K = -\frac{4}{\pi\sigma} \int_{-c/2}^{c/2} H_y^{(i)}(0, y, 0) H_y(0, y, 0) dy - \frac{4}{\pi\sigma} \int_{-c/2}^{c/2} H_y^{(i)}(0, y, 0) H_{y\text{TM}}(0, y, 0) dy + \frac{1}{\sigma} \int_{-c/2}^{c/2} \frac{1}{\cos\theta} H_y^{(i)}(0, y, 0) H_{r\text{TM}}(0, y, z_e) dy. \quad (67)$$

D. Summary

The change in impedance in an eddy-current coil due to a surface crack is given by

$$\Delta Z = Z_S + Z_F + Z_K, \quad (68)$$

where Z_S is given in Eq. (52), Z_F is given in Eq. (61) and Z_K is given in Eq. (67). These expressions involve simple one-dimensional integrals along the line of the crack mouth. The development of Z_S and Z_F is rigorous and these terms pro-

vide the full contribution to ΔZ at the order of the first two terms in Eq. (3). The derivation of Z_K is not as rigorous but it provides a good approximation to the third term in Eq. (3).

V. LONG CRACK

The solution for a long, surface defect of uniform depth is most readily obtained by Fourier transforming in the direction of the line followed by the crack. For the purpose of calculating the fields, let the crack occupy $x=0, -\infty < y < \infty, -d \leq z \leq 0$, as shown in Figure 6, and let $\tilde{\psi}(v, z)$ be the Fourier transform of $\psi(y, z)$ in y . The solution of the Fourier transform of Eq. (13), which vanishes at $z = -d$ in accordance with Eq. (21), has the form

$$\tilde{\psi}(v, z) = A(v) \sinh[v(z + d)]. \quad (69)$$

The coefficient $A(v)$ is determined from the boundary condition at the crack mouth. Fourier transforming Eq. (24) yields

$$\left. \frac{\partial \tilde{\psi}(v, z)}{\partial z} \right|_{z=0} = \tilde{H}_{y\text{TM}}^{(i)}(v, 0) - \frac{2v^2}{ik} \tilde{U}(v) \tilde{\psi}(v, 0), \quad (70)$$

where $\tilde{U}(v)$ is given in Eq. (32), and hence

$$\tilde{\psi}(v, z) = \frac{\sinh[v(z + d)]}{v \cosh(vd) [1 + 2(v/ik) \tilde{U}(v) \tanh(vd)]} \times \tilde{H}_{y\text{TM}}^{(i)}(v, 0). \quad (71)$$

The effect of including $H_{y\text{TM}}^{(s)}$ in the boundary condition given in Eq. (22) is now clear. It gives rise to the term $2(v/ik) \tilde{U}(v) \tanh(vd)$ in the denominator of Eq. (71), which depends on μ_r through $\tilde{U}(v)$.

If $\tilde{H}_y(v)$ is the Fourier transform of $H_y(y)$ in y , then Fourier transforming Eq. (28) gives

$$\tilde{H}_y(v) = \tilde{H}_y^{(i)}(v) + 2 \frac{v^2}{ik} \tilde{V}(v) \tilde{\psi}(v), \quad (72)$$

where $\tilde{H}_y(v) = \tilde{H}_y(0, v, 0)$, etc., and $\tilde{V}(v)$ is given in Eq. (37). Substituting for $\tilde{\psi}$ from Eq. (71) and making the thin-skin approximation¹⁴

$$\tilde{H}_{y\text{TM}}^{(i)} \approx \tilde{H}_y^{(i)}, \quad (73)$$

gives

$$\tilde{H}_y(v) = \frac{1 + 2(v/ik) [\tilde{U}(v) + \tilde{V}(v)] \tanh(vd)}{1 + 2(v/ik) \tilde{U}(v) \tanh(vd)} \tilde{H}_y^{(i)}(v). \quad (74)$$

From Eqs. (33) and (38) it is clear that, for $\mu_r \gg 1$, \tilde{U} and \tilde{V} are equal and opposite so that

$$\tilde{H}_y(v)_{\mu_r \gg 1} = \frac{1}{1 + 2(v/ik) \tilde{U}_{\mu_r \gg 1}(v) \tanh(vd)} \tilde{H}_y^{(i)}(v). \quad (75)$$

The impedance change due to a long slot can now be calculated by Fourier transforming Eqs. (52) and (61) using

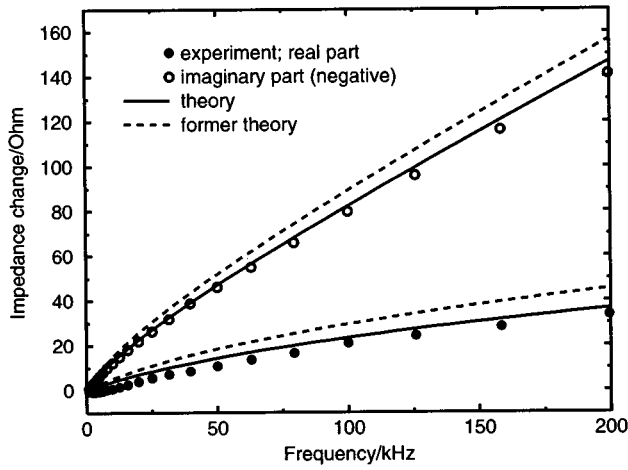


FIG. 7. Impedance predictions and experimental data for a coil centred over a long slot in aluminium. The broken lines represent predictions made using Auld's assumption that the tangential magnetic field at the conductor surface is undisturbed by a surface defect (see Ref. 1).

Parseval's theorem. Note that if third-order contributions to ΔZ are required, the approximation of Eq. (73) should not be used since it has a third-order effect.

VI. PREDICTIONS AND EXPERIMENTAL DATA

In Figures 7 and 8, impedance predictions are compared with experimental data from frequency scans for coils centred over long slots in aluminium and steel, respectively. Predictions are made at the order of the first two terms in Eq. (3), involving the expressions for Z_S and Z_F given in Eqs. (52) and (61). The experimental parameters are given in Table I. In comparing theoretical predictions with data for a slot in aluminium, we show the improvement obtained by retaining the scattered field term $H_{yTM}^{(s)}$ in Eq. (22). Predictions made using Auld's approximation,^{1,9} in which this term is neglected, are shown as dashed lines in Figure 7 and represent an over prediction of about 15% in $|\Delta Z|$ for frequen-

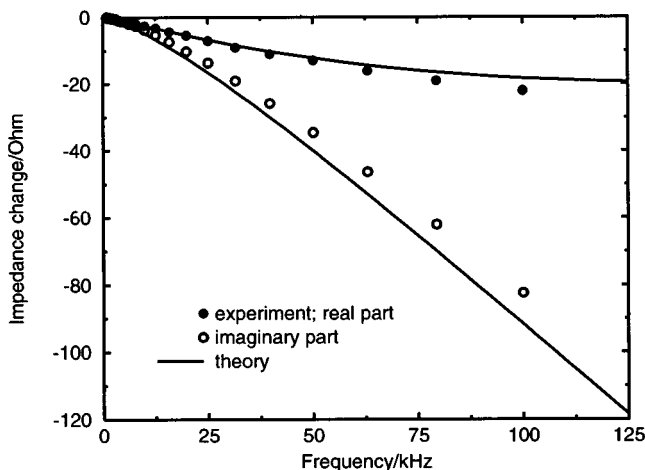


FIG. 8. Impedance predictions and experimental data for a coil centred over a long slot in mild steel.

TABLE I. Experimental parameters.

Material	Type	Aluminium	Mild steel
	σ/Sm^{-1}	1.667×10^7	5.587×10^6
	μ_r	1	87 ± 5
Defect	Depth/mm	11.99	2.95 ± 0.05
	Gape/mm	0.41 ± 0.08	0.33 ± 0.03
Coil	Inner radius/mm	3.015	
	Outer radius/mm	5.46	
	Length/mm	2.94	
	lift-off/mm	1.32	1.29
	No. of turns	900	
	Free-space inductance/mH	6.027	
	Resonant frequency/kHz	850	

cies above 50 kHz. The theory presented here predicts $|\Delta Z|$ to within 5%, which is the level of experimental error in the measurements. Note that the strength of the scattered field term depends on the ratio of the coil diameter to the crack depth. As this ratio increases, the predictions of Auld's theory and the theory presented here converge. The effect of omitting terms of order of the third term in Eq. (3) can be seen in the over prediction of $\text{Re}(\Delta Z)$ at frequencies below about 50 kHz. This discrepancy between theory and experiment can be largely eliminated by including the Kahn level terms in the predictions.

Theoretical predictions of the coil impedance change due to a slot in mild steel, shown in Figure 8, agree with experimental data to within 10% for $|\Delta Z|$. The error is larger than for the slot in aluminium, and may in part be attributed to the difficulty associated with measuring μ_r experimentally. It is likely that the permeability of material near the slot faces differs from that of the bulk as a result of surface damage occurring during the manufacture of the slot. In practice, it is the value of the bulk permeability which is measured and used to make the predictions of impedance change. In Figure 9, predictions are shown for a system identical to that of Figure 8 but with different values of material permeability. The impedance change depends on μ_r in a

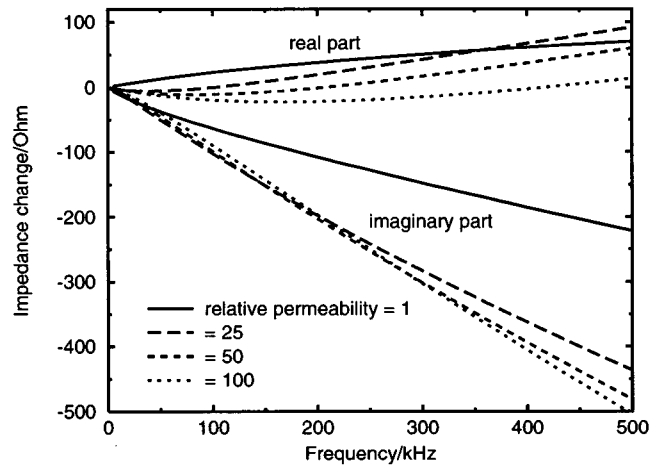


FIG. 9. Predicted coil impedance change due to a long slot in materials of different permeability.

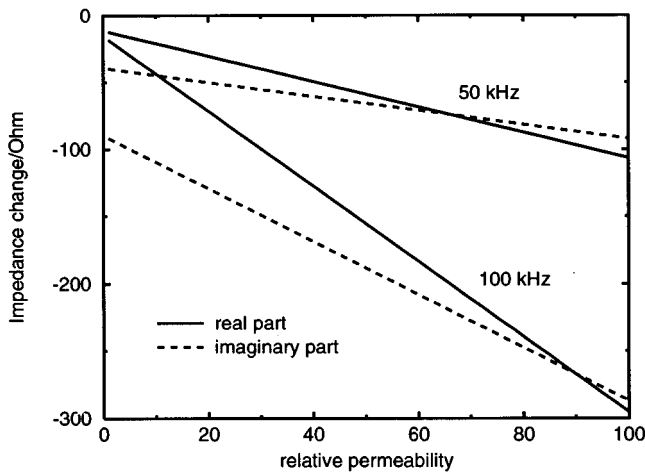


FIG. 10. Variation in the predicted coil impedance change due to a long slot as the relative permeability of the material filling the slot is varied.

complicated manner but from Figure 9 it can be seen that increasing the value of μ_r in the theory would improve the fit to the data in Figure 8.

Finally we demonstrate the effect of varying the relative permeability of the material within the slot. In practice, defects may be filled with oxide deposits which can be electrically conducting and permeable. Predictions of coil impedance change are shown in Figure 10 for the defect of Figure 8 filled with material which is non-conducting but permeable. It is evident that $|\Delta Z|$ increases as μ_c increases. This is a consequence of the form of the term of order k^2 (the volume-dependent term) in Eq. (61). This result is consistent with previous work which has shown that impedance predictions for air-filled defects in steel are relatively insensitive to the defect gape.¹⁵ It can be seen that this is the case by putting $\mu_c = 1$ and μ_r large in Eq. (61). For a typical crack in which the gape is much smaller than the depth, the term of order k^2 is then likely to be much smaller than that of order k in the first term of Eq. (61), rendering $|\Delta Z|$ relatively insensitive to a .

VII. CONCLUSION

A theory capable of predicting the impedance change in an eddy-current probe due to surface cracks in materials of arbitrary permeability is presented. The theory is valid in the high-frequency regime, in which the electromagnetic skin depth is significantly smaller than the crack dimensions and the induced currents flow in a thin skin at the surface of the conductor and at the faces of the crack.

The electromagnetic field induced by an eddy-current coil in a typical conductor interacts with a defect predominantly via the electric field. For a circular coil whose axis is centred over the plane of a crack, the normal component of the magnetic field is zero at the crack and the interaction between the induced field and the defect occurs purely via the electric field. For a coil whose axis is offset from the crack plane, however, there is some interaction between the magnetic field and the defect. The effect of this interaction is quite noticeable for slots with large gape in strongly mag-

netic conductors, since the magnetic flux tends to remain within the conductor rather than pass into the air gap in the defect, but is negligible in non-magnetic materials. This work considers only the interaction between the electric field and the defect. The solution is exact for circular coils centred over the crack but predictions for coils offset from air-filled slots in magnetic materials could be improved by including the interaction between the magnetic field and the defect.

The impedance change in a coil is expressed as a power series in the small parameter $1/ik$ and new forms for the first three terms in this series are derived. They are expressed as one-dimensional integrals along the line of the crack mouth. These integrals can be evaluated quickly, taking a few seconds per point using a personal computer, and predictions have been compared with experimental data for coils centred over long slots in aluminium and mild steel. Good agreement is observed.

ACKNOWLEDGMENTS

This work was supported by Nuclear Electric Ltd. and Magnox Electric plc, UK. The authors gratefully acknowledge provision of the experimental data by Dr. S. K. Burke of the DSTO Aeronautical and Maritime Research Laboratory, Melbourne, Australia.

APPENDIX: HALF-SPACE FIELD ANALYSIS BY SCALAR DECOMPOSITION

Consider the electromagnetic field in a problem domain divided into two semispaces at the plane $z=0$. The upper half space is non-conducting and the lower half space has a uniform conductivity σ . The field is to be expressed in terms of TE and TM potentials defined with respect to different preferred directions in the two regions. In the upper half space, region 1, the preferred direction is normal to the interface between the conducting and non-conducting regions. In the lower half space the preferred direction is tangential to the interface. For convenience, the coordinate system is chosen such that the preferred direction in the conducting region, region 2, is the x direction.

In homogeneous isotropic regions the TE and TM potentials obey independent equations but, because different preferred directions are used in the two half spaces, cross coupling occurs between the respective modes at the interface. The effect of this cross coupling is embodied in a 2×2 matrix of interface transmission and reflection coefficients which allow, for example, a TE mode to be reflected by an incident TM mode and vice versa.

The mode coupling is built into a set of half-space scalar Green's functions that are defined below following a preliminary analysis which determines the transmission and reflection coefficients. The coefficients are derived for an arbitrary source in the conductor using a two-dimensional Fourier transform of the field. Then the scalar Green's functions are found as a special case by considering singular sources.

A. Scalar decomposition

Assuming a time dependence $\exp(-i\omega t)$, the electric field in the non-conducting region, region 1, may be expressed using a TE potential ψ'_1 and a TM potential ψ''_1 :^{10,16}

$$\mathbf{E}(\mathbf{r}) = i\omega\mu_0[\nabla \times \hat{z}\psi'_1(\mathbf{r}) - \nabla \times \nabla \times \hat{z}\psi''_1(\mathbf{r})], \quad z > 0, \quad (\text{A1})$$

where \hat{z} is a unit vector normal to the plane of the interface defined by $z=0$. Similarly, the electric field in the conducting region will be represented as

$$\mathbf{E}(\mathbf{r}) = i\omega\mu[\nabla \times \hat{x}\psi'_2(\mathbf{r}) - \nabla \times \nabla \times \hat{x}\psi''_2(\mathbf{r})], \quad z < 0, \quad (\text{A2})$$

where \hat{x} is a unit vector tangential to the conductor surface and $\mu = \mu_0\mu_r$, where μ_r is the relative permeability of the conductor. In terms of the TM and TE potentials, the magnetic field in each region is given by

$$\mathbf{H}(\mathbf{r}) = \nabla \times \nabla \times \hat{z}\psi'_1(\mathbf{r}), \quad z > 0 \quad (\text{A3})$$

and

$$\mathbf{H}(\mathbf{r}) = \nabla \times \nabla \times \hat{x}\psi'_2(\mathbf{r}) - k^2\nabla \times \hat{x}\psi''_2(\mathbf{r}), \quad z < 0. \quad (\text{A4})$$

Using Maxwell's equations it can be shown that

$$\nabla^2\nabla_z^2\psi_1(\mathbf{r}) = 0, \quad z > 0, \quad (\text{A5})$$

$$(\nabla^2 + k^2)\nabla_x^2\psi_2(\mathbf{r}) = 0, \quad z < 0, \quad (\text{A6})$$

where it is implicit that the ψ_i carry either a single or double prime, depending on whether they represent the TE or the TM potential, respectively, $i=1,2$,

$$\nabla_x = \nabla - \hat{x} \frac{\partial}{\partial x} \quad \text{and} \quad \nabla_z = \nabla - \hat{z} \frac{\partial}{\partial z}. \quad (\text{A7})$$

Equations for the coefficients which couple the TE and TM potentials at the interface between regions 1 and 2 are found through consideration of the field continuity conditions at the interface;

$$\hat{z} \times \mathbf{E}(\mathbf{r}_1) = \hat{z} \times \mathbf{E}(\mathbf{r}_2), \quad (\text{A8})$$

$$\hat{z} \times \mathbf{H}(\mathbf{r}_1) = \hat{z} \times \mathbf{H}(\mathbf{r}_2), \quad (\text{A9})$$

where \mathbf{r}_1 and \mathbf{r}_2 represent limiting values of the field coordinates at the interface as it is approached from above and below, respectively. These equations express the continuity of tangential electric and magnetic field components across the boundary. The coupling coefficients are most conveniently found by using the two-dimensional Fourier transform with respect to the x and y coordinates. Define

$$\tilde{F}(u, v, z) = \int_{-\infty}^{\infty} \int_{-\infty}^{\infty} F(\mathbf{r}) e^{-i(ux+vy)} dx dy, \quad (\text{A10})$$

where u and v are Fourier space coordinates. Transforming Eqs. (A5) and (A6) using Eq. (A10) reveals that ψ_1 and ψ_2 obey the following second-order differential equations in z :

$$\left(\frac{\partial^2}{\partial z^2} - \kappa^2 \right) \tilde{\psi}_1(u, v, z) = 0, \quad z > 0, \quad (\text{A11})$$

$$\left(\frac{\partial^2}{\partial z^2} - \gamma^2 \right) \tilde{\psi}_2(u, v, z) = 0, \quad z < 0, \quad (\text{A12})$$

where $\kappa = (u^2 + v^2)^{1/2}$, $\gamma = (u^2 + v^2 - k^2)^{1/2}$ and roots with positive real parts are taken.

B. Internal source

The precise nature of the coupling between the TM and TE potentials at the interface between regions 1 and 2 will now be established for a source within the conductor. The solution of Eq. (A11), vanishing as $z \rightarrow \infty$, may be written

$$\begin{bmatrix} \tilde{\psi}'_1(u, v, z) \\ \tilde{\psi}''_1(u, v, z) \end{bmatrix} = \begin{bmatrix} c' \\ c'' \end{bmatrix} e^{-\kappa z}. \quad (\text{A13})$$

The solution of Eq. (A12) in the region above the source but below the surface of the conductor has the form

$$\begin{bmatrix} \tilde{\psi}'_2(u, v, z) \\ \tilde{\psi}''_2(u, v, z) \end{bmatrix} = \begin{bmatrix} a' \\ a'' \end{bmatrix} e^{-\gamma z} + \begin{bmatrix} b' \\ b'' \end{bmatrix} e^{\gamma z}. \quad (\text{A14})$$

The first term on the right-hand side of Eq. (A14) represents the free-space solution in the conductor, the a^i are source-dependent coefficients, $i = ' \text{ or } ''$. The b^i and c^i are related to the a^i via reflection and transmission coefficients which are found by using the field continuity conditions at the conductor surface, Eqs. (A8) and (A9). In some special cases there is no cross coupling between TM and TE potentials at the conductor surface but in general the possibility must be allowed for. This allowance can be made by defining the following relationships between the coefficients in Eqs. (A13) and (A14):

$$\begin{bmatrix} b' \\ b'' \end{bmatrix} = \begin{bmatrix} \Gamma_{11} & \Gamma_{12} \\ \Gamma_{21} & \Gamma_{22} \end{bmatrix} \begin{bmatrix} a' \\ a'' \end{bmatrix}, \quad (\text{A15})$$

$$\begin{bmatrix} c' \\ c'' \end{bmatrix} = \begin{bmatrix} T_{11} & T_{12} \\ T_{21} & T_{22} \end{bmatrix} \begin{bmatrix} a' \\ a'' \end{bmatrix}, \quad (\text{A16})$$

where the Γ_{ij} ($i, j=1,2$) are reflection coefficients and the T_{ij} are transmission coefficients. Using Eqs. (A2) and (A4) it is found that

$$-iuc' + iv\kappa c'' = \mu_r \gamma [a' - b'] - \mu_r uv [a'' + b''], \quad (\text{A17})$$

$$-ivc' - iu\kappa c'' = \mu_r (u^2 - k^2) [a'' + b''], \quad (\text{A18})$$

$$-iv\kappa c' = uv [a' + b'] - \gamma k^2 [a'' - b''], \quad (\text{A19})$$

$$iu\kappa c' = -(u^2 - k^2) [a' + b']. \quad (\text{A20})$$

Expressing the solution of these equations in the form of Eqs. (A15) and (A16) gives

$$D\Gamma_{11} = -\gamma\kappa(u^2 - k^2) + \mu_r(\gamma^2 u^2 + k^2 v^2), \quad (\text{A21})$$

$$D\Gamma_{12} = -2\mu_r \gamma k^2 uv,$$

$$D\Gamma_{21} = -2\mu_r \gamma uv, \quad (\text{A22})$$

$$D\Gamma_{22} = \gamma\kappa(u^2 - k^2) + \mu_r(\gamma^2 u^2 + k^2 v^2)$$

and

$$DT_{11} = -\frac{2\mu_r \gamma^2 u(u^2 - k^2)}{i\kappa},$$

$$DT_{12} = \frac{2\mu_r \gamma k^2 v (u^2 - k^2)}{i\kappa}, \quad (\text{A23})$$

$$DT_{21} = \frac{2\mu_r \gamma v (\gamma + \mu_r \kappa) (u^2 - k^2)}{i\kappa^2}, \quad (\text{A24})$$

$$DT_{22} = -\frac{2\mu_r \gamma^2 u (\gamma + \mu_r \kappa) (u^2 - k^2)}{i\kappa^2},$$

where

$$D = \kappa (\gamma + \mu_r \kappa) (u^2 - k^2). \quad (\text{A25})$$

Note that Γ_{22} can be written

$$\Gamma_{22} = 1 + \frac{2\mu_r v^2 k^2}{D}, \quad (\text{A26})$$

which demonstrates clearly that the nature of the reflection at the boundary reduces to a simple image when the spatial frequency in the y direction is nugatory.

C. Scalar Green's functions

In principle, a solution for the ψ_i in the form

$$\begin{bmatrix} \psi'_1(\mathbf{r}) \\ \psi''_2(\mathbf{r}) \end{bmatrix} = \int \begin{bmatrix} U_{11}(\mathbf{r}, \mathbf{r}_0) & U_{12}(\mathbf{r}, \mathbf{r}_0) \\ U_{21}(\mathbf{r}, \mathbf{r}_0) & U_{22}(\mathbf{r}, \mathbf{r}_0) \end{bmatrix} \begin{bmatrix} j'(\mathbf{r}_0) \\ j''(\mathbf{r}_0) \end{bmatrix} d\mathbf{r}_0 \quad (\text{A27})$$

is sought. However, for the specific crack problem at hand, a surface integral is to be formed using Green's second theorem which means that the precise forms of the volumetric scalar sources $j'(\mathbf{r})$ and $j''(\mathbf{r})$ are not needed. The coupled Green's functions required satisfy

$$\nabla^2 \begin{bmatrix} G_{11}(\mathbf{r}, \mathbf{r}_0) & G_{12}(\mathbf{r}, \mathbf{r}_0) \\ G_{21}(\mathbf{r}, \mathbf{r}_0) & G_{22}(\mathbf{r}, \mathbf{r}_0) \end{bmatrix} = \begin{bmatrix} 0 & 0 \\ 0 & 0 \end{bmatrix}, \quad z > 0, \quad (\text{A28})$$

$$\begin{aligned} & (\nabla^2 + k^2) \begin{bmatrix} G_{11}(\mathbf{r}, \mathbf{r}_0) & G_{12}(\mathbf{r}, \mathbf{r}_0) \\ G_{21}(\mathbf{r}, \mathbf{r}_0) & G_{22}(\mathbf{r}, \mathbf{r}_0) \end{bmatrix} \\ & = -\delta(\mathbf{r} - \mathbf{r}_0) \begin{bmatrix} 1 & 0 \\ 0 & 1 \end{bmatrix}, \quad z < 0, \end{aligned} \quad (\text{A29})$$

with

$$\lim_{|\mathbf{r}| \rightarrow \infty} G_{ij} = 0, \quad i, j = 1, 2. \quad (\text{A30})$$

The functions $U_{ij}(\mathbf{r}, \mathbf{r}_0)$ are related to the Green's functions by

$$G_{ij}(\mathbf{r}, \mathbf{r}_0) = -\nabla_z^2 U_{ij}(\mathbf{r}, \mathbf{r}_0), \quad z > 0, \quad (\text{A31})$$

$$G_{ij}(\mathbf{r}, \mathbf{r}_0) = -\nabla_x^2 U_{ij}(\mathbf{r}, \mathbf{r}_0), \quad z < 0. \quad (\text{A32})$$

Imposing the same interface conditions on the $U_{ij}(\mathbf{r}, \mathbf{r}_0)$ as apply to their corresponding potentials makes the $U_{ij}(\mathbf{r}, \mathbf{r}_0)$ become, in effect, the potential due to a singular source at \mathbf{r}_0 .

Defining

$$\tilde{G}_{ij}(z, z_0) = \int_{-\infty}^{\infty} \int_{-\infty}^{\infty} G_{ij}(\mathbf{r}, \mathbf{r}_0) e^{-iu(x-x_0) - iv(y-y_0)} dx dy, \quad (\text{A33})$$

$i, j = 1, 2$, allows the transformation of Eqs. (A28) and (A29), giving

$$\left(\frac{\partial^2}{\partial z^2} - \kappa^2 \right) \begin{bmatrix} \tilde{G}_{11}(z, z_0) & \tilde{G}_{12}(z, z_0) \\ \tilde{G}_{21}(z, z_0) & \tilde{G}_{22}(z, z_0) \end{bmatrix} = \begin{bmatrix} 0 & 0 \\ 0 & 0 \end{bmatrix}, \quad z > 0, \quad (\text{A34})$$

$$\begin{aligned} & \left(\frac{\partial^2}{\partial z^2} - \gamma^2 \right) \begin{bmatrix} \tilde{G}_{11}(z, z_0) & \tilde{G}_{12}(z, z_0) \\ \tilde{G}_{21}(z, z_0) & \tilde{G}_{22}(z, z_0) \end{bmatrix} \\ & = -\delta(z - z_0) \begin{bmatrix} 1 & 0 \\ 0 & 1 \end{bmatrix}, \quad z < 0. \end{aligned} \quad (\text{A35})$$

Using the same two-dimensional Fourier transformation, Eqs. (A31) and (A32) become

$$\tilde{G}_{ij}(z, z_0) = \kappa^2 \tilde{U}_{ij}(z, z_0), \quad z > 0, \quad (\text{A36})$$

$$\tilde{G}_{ij}(z, z_0) = -\left(\frac{\partial^2}{\partial z^2} - v^2 \right) \tilde{U}_{ij}(z, z_0), \quad z < 0. \quad (\text{A37})$$

The reflection and transmission coefficients given above will now be used to construct half-space Green's functions for the potentials. The form of \tilde{G}_{ii} must reflect the presence of the singular source at $z = z_0$. Let \tilde{G}_0 be an unbounded domain scalar Green's function which exhibits the following behavior:

$$\left[\frac{\partial \tilde{G}_0}{\partial z} \right]_{z=z_0+} - \left[\frac{\partial \tilde{G}_0}{\partial z} \right]_{z=z_0-} = -1, \quad (\text{A38})$$

$$[\tilde{G}_0]_{z=z_0+} - [\tilde{G}_0]_{z=z_0-} = 0. \quad (\text{A39})$$

The general solution for \tilde{G}_0 is of the form

$$\tilde{G}_0 = \begin{cases} A(\gamma) e^{-\gamma(z-z_0)}, & z > z_0 \\ B(\gamma) e^{\gamma(z-z_0)}, & z < z_0 \end{cases}. \quad (\text{A40})$$

Applying Eqs. (A38) and (A39) to Eq. (A40) yields

$$\tilde{G}_0 = \frac{1}{2\gamma} e^{-\gamma|z-z_0|}. \quad (\text{A41})$$

The source term contained in \tilde{G}_{ii} is, therefore, given by Eq. (A41). Comparing Eqs. (A41) and (A32) with Eq. (A14) allows the deduction that

$$a' = a'' = -\frac{1}{2\gamma(u^2 - k^2)} e^{\gamma z_0} \quad (\text{A42})$$

for a singular source at z_0 where $z_0 < z$. In addition to the singular term, the \tilde{G}_{ii} contain non-singular terms which represent the reflection, at the conductor surface, of the outgoing "wave" from the source. From Eqs. (A14)–(A16) and Eq. (A41) it is found that

$$\begin{aligned} & \begin{bmatrix} \tilde{G}_{11}(z, z_0) & \tilde{G}_{12}(z, z_0) \\ \tilde{G}_{21}(z, z_0) & \tilde{G}_{22}(z, z_0) \end{bmatrix} \\ & = -\frac{\kappa^2}{2\gamma(u^2 - k^2)} \begin{bmatrix} T_{11} & T_{12} \\ T_{21} & T_{22} \end{bmatrix} e^{\gamma(z+z_0)}, \quad z > 0, \end{aligned} \quad (\text{A43})$$

$$\begin{bmatrix} \tilde{G}_{11}(z, z_0) & \tilde{G}_{12}(z, z_0) \\ \tilde{G}_{21}(z, z_0) & \tilde{G}_{22}(z, z_0) \end{bmatrix} = \frac{1}{2\gamma} \left\{ \begin{bmatrix} 1 & 0 \\ 0 & 1 \end{bmatrix} e^{-\gamma|z-z_0|} + \begin{bmatrix} \Gamma_{11} & \Gamma_{12} \\ \Gamma_{21} & \Gamma_{22} \end{bmatrix} e^{\gamma(z+z_0)} \right\}, \quad z < 0. \quad (\text{A44})$$

Assuming that the \tilde{G}_{ij} and the \tilde{U}_{ij} have the same z dependence, Eq. (A37) can be written

$$\tilde{G}_{ij}(u, v, z, z_0) = -(u^2 - k^2) \tilde{U}_{ij}(u, v, z, z_0) \quad z < 0. \quad (\text{A45})$$

The Green's functions can now be related to the functions \tilde{U}_{ij} by means of Eqs. (A36) and (A45):

$$\begin{bmatrix} \tilde{U}_{11}(z, z_0) & \tilde{U}_{12}(z, z_0) \\ \tilde{U}_{21}(z, z_0) & \tilde{U}_{22}(z, z_0) \end{bmatrix} = -\frac{1}{2\gamma(u^2 - k^2)} \begin{bmatrix} T_{11} & T_{12} \\ T_{21} & T_{22} \end{bmatrix} e^{\gamma(z+z_0)}, \quad z > 0, \quad (\text{A46})$$

$$\begin{bmatrix} \tilde{U}_{11}(z, z_0) & \tilde{U}_{12}(z, z_0) \\ \tilde{U}_{21}(z, z_0) & \tilde{U}_{22}(z, z_0) \end{bmatrix} = -\frac{1}{2\gamma(u^2 - k^2)} \left\{ \begin{bmatrix} 1 & 0 \\ 0 & 1 \end{bmatrix} e^{-\gamma|z-z_0|} + \begin{bmatrix} \Gamma_{11} & \Gamma_{12} \\ \Gamma_{21} & \Gamma_{22} \end{bmatrix} e^{\gamma(z+z_0)} \right\}, \quad z < 0. \quad (\text{A47})$$

These functions satisfy the field continuity conditions on the interface between the two regions.

¹B. A. Auld, S. R. Jefferies, and J. C. Moulder, *J. Nondestruct. Eval.* **7**, 79 (1988).

²A. M. Lewis, D. H. Michael, M. C. Lugg, and R. Collins, *J. Appl. Phys.* **64**, 3777 (1988).

³S. K. Burke, *J. Appl. Phys.* **76**, 3072 (1994).

⁴A. M. Lewis, *J. Phys. D* **25**, 319 (1992).

⁵R. Collins, W. D. Dover, and D. H. Michael, in *Research Techniques in Nondestructive Testing*, edited by R. S. Sharpe (Academic, London, 1985), Vol. 8, Chap. 5.

⁶A. H. Kahn, R. Spal, and A. Feldman, *J. Appl. Phys.* **48**, 4454 (1977).

⁷N. Harfield and J. R. Bowler, *J. Appl. Phys.* **76**, 4853 (1994).

⁸C. V. Dodd and W. E. Deeds, *J. Appl. Phys.* **39**, 2829 (1968).

⁹B. A. Auld, F. G. Muenneemann, and M. Riazat, in *Research Techniques in Nondestructive Testing*, 1984, Vol. 7, Chap. 2.

¹⁰L. B. Felsen and N. Marcuvitz, *Radiation and Scattering of Waves* (Prentice-Hall, Englewood Cliffs, NJ, 1973).

¹¹J. R. Bowler, *J. Appl. Phys.* **75**, 8128 (1994).

¹²J. R. Bowler, Y. Yoshida, and N. Harfield, *IEEE Trans. Magn.* (accepted).

¹³N. Harfield and J. R. Bowler, in *Review of Progress in Quantitative NDE*, edited by D. O. Thompson and D. E. Chimenti (Plenum, New York, 1997), Vol. 16, p. 241.

¹⁴It can be shown that

$$\tilde{H}_{y\text{TM}}^{(i)}(u, v, z) = \frac{k^2}{k^2 - u^2} \tilde{H}_y^{(i)}(u, v, z),$$

where $\tilde{H}_{y\text{TM}}^{(i)}(u, v, z)$ is the two-dimensional Fourier transform of $H_{y\text{TM}}^{(i)}(x, y, z)$. In the thin-skin limit, the spatial frequency u is typically much smaller than k . Putting $u^2 \ll k^2$ in the above gives Eq. (73).

¹⁵R. E. Beissner, *J. Nondestruct. Eval.* **13**, 175 (1994).

¹⁶J. A. Stratton, *Electromagnetic Theory* (McGraw-Hill, New York, 1941).